Organic & Biomolecular Chemistry

ROYAL SOCIETY OF CHEMISTRY

PAPER

View Article Online
View Journal | View Issue

Cite this: *Org. Biomol. Chem.*, 2021, **19**, 406

Carbazole-modified thiazolo[3,2-*c*][1,3,5,2]oxadiazaborinines exhibiting aggregation-induced emission and mechanofluorochromism†

Mykhaylo A. Potopnyk, *[a,b] Mykola Kravets, [c] Roman Luboradzki,[c] Dmytro Volyniuk, [b] Volodymyr Sashuk [c] and Juozas Vidas Grazulevicius *[b]

Received 8th November 2020,
Accepted 1st December 2020

DOI: 10.1039/d0ob02225j

rsc.li/obc

Two highly emissive carbazole-containing thiazole-fused oxadiazaborinines were designed and synthesized. These *N*,*O*-chelated organoboron dyes displayed large Stokes shifts and remarkable solvatofluorochromism in solutions, as well as good thermal stability and comparatively high photoluminescence quantum yields (up to 34%) in the solid state. The presence of a carbazole donor unit, linked with the oxadiazaborinine acceptor *via* a phenyl linker, restricted intramolecular rotation, leading to enhanced aggregation-induced emission properties of the compounds: in THF/water mixtures with a large water percentage, they demonstrated the formation of emissive nanoaggregates with an average size of 79 and 89 nm for complexes **2** and **3**, respectively. The introduction of bulky *tert*-butyl groups attached to the carbazole moiety induced significant mechanofluorochromic properties of the compounds.

Introduction

The development of organic compounds exhibiting aggregation-induced emission (AIE) has become a very active research field in the bioimaging area, materials sciences and supramolecular chemistry.[1] Numerous AIE-active luminogens (AIEgens) have been widely applied as photosensitisers in photodynamic therapy,[2] fluorescent probes,[3] emitters in optoelectronic devices,[4] components of liquid crystalline materials,[5] supramolecular systems,[6] fluorescent gels,[7] *etc*. The most efficient strategy to achieve the AIE properties is the introduction of propeller-shaped or bulky functional groups to the fluorophore structures, which moderately restricts their intramolecular motion in the aggregated state. This in turn results in an increased photoluminescence quantum yield (PLQY) in the aggregated state caused by the reduction of nonradiative energy dissipation.[1] Currently, the most well-known AIEgens are tetraphenylethylene derivatives.[1,2a,c,3b,c,4e,6a,b,7,8] Meanwhile, in the case of donor–acceptor type dyes, the bulky donor moieties, such as triphenylamine,[2b–e,3a,d,9] carbazole,[3e,4d,9c,10] 9,10-dihydroacridine,[4c,d] phenoxazine,[4d] or phenothiazine,[4a] have been utilized to enhance the AIE ability of fluorophores.

Among luminescent compounds, organoboron complexes are especially valuable due to their advantages such as strong absorption bands in the UV-vis region, intensive emission, high PLQYs in solutions, photochemical stability, *etc*.[11] To date, the most famous organoboron complexes have been boron-dipyrromethenes (BODIPYs).[11a–d] However, due to the C_2-symmetry of the BODIPY core, such dyes usually exhibit small values of Stokes shifts, which in turn lead to the low solid-state emissive ability. This substantially restrains the elaboration of BODIPY-based AIEgens.[9b,12] The effective strategies to design AIE-active organoboron complexes include desymmetrisation of the fluorophore scaffold.[12,13] From this point of view, *N*,*O*-coordinated organoboron dyes, because of their unsymmetrical nature, look very promising.[3a,9a,13a–h] However, to date, it remains challenging to design AIE-active organoboron dyes with high solid-state PLQYs.

Recently, we have described the new highly emissive difluoroboron complex **1** (Fig. 1), which is based on a thiazolo[3,2-*c*]oxadiazaborinine core conjugated with a dimethylamino donor group *via* a rotatable phenyl linker.[14]

Compound **1** exhibited high chemical stability and could be easily modified in the thiazole unit.[14d] However, despite the AIE activity of complex **1**, the thiazole-modified analogues exhibited aggregation-caused quenching (ACQ) of emission.[14] Meanwhile, the design of thiazolo[3,2-*c*]oxadiazaborinines with enhanced AIE properties could open the way to the widespread application of such dyes.

[a]*Institute of Organic Chemistry, Polish Academy of Sciences, Kasprzaka 44/52, 01-224 Warsaw, Poland. E-mail: potopnyk@gmail.com, mykhaylo.potopnyk@icho.edu.pl*
[b]*Department of Polymer Chemistry and Technology, Kaunas University of Technology, Radvilenu pl. 19, LT-50254 Kaunas, Lithuania. E-mail: juozas.grazulevicius@ktu.lt*
[c]*Institute of Physical Chemistry, Polish Academy of Sciences, Kasprzaka 44/52, 01-224 Warsaw, Poland*

† Electronic supplementary information (ESI) available. CCDC 2013916 for **2**. For ESI and crystallographic data in CIF or other electronic format see DOI: 10.1039/d0ob02225j

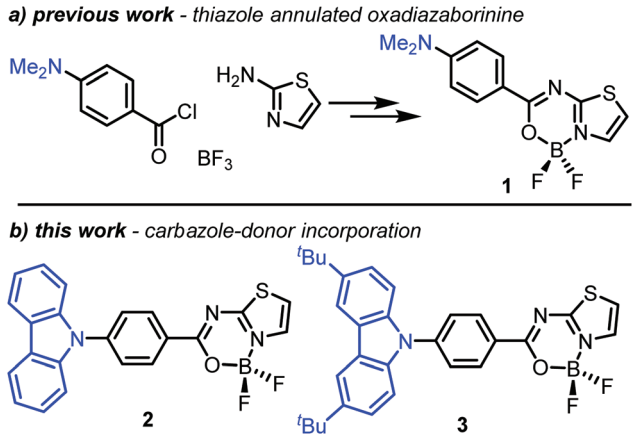

Fig. 1 (a) Previous work: design of thiazole annulated oxadiazaborinine **1**; (b) structures of carbazole-containing thiazolo-oxadiazaborinines **2** and **3**.

Herein, we demonstrate that the replacement of the Me_2N-group by the carbazole moiety (dyes **2** and **3**) which results in the remarkable increase of solvatofluorochromism, and, due to the restriction of intramolecular rotation, in enhanced AIE activity. Strikingly, the attachment of two ^{t}Bu groups to the carbazole unit (dye **3**) induced significant mechanofluorochromic properties. The important advantages of compounds **2** and **3**, compared with other *N*,*O*-coordinating difluoroborons, are synthetic availability, high thermal stability, large values of Stokes shifts and relatively high solid-state PLQYs.

Results and discussion

Synthesis and characterization

Complexes **2** and **3** were successfully synthesized in four steps, starting from commercially available carbazole (**4**) and 3,6-di-*tert*-butylcarbazole (**5**), which was obtained by standard *tert*-butylation[15] of substrate **4** in 85% yield (Scheme 1). Carbazoles **4** and **5** were coupled with ethyl 4-iodobenzoate (**6**) in the presence of CuI/1,10-phenanthroline/K_2CO_3 or Cu_2O in refluxed dimethylacetamide (DMA) giving products **7** and **8** in 80 and 95% yields, respectively. Next, after hydrolysis of the ester group, 4-(9*H*-carbazol-9-yl)benzoic acid (**9**) and 4-(3,6-di-*tert*-butyl-9*H*-carbazol-9-yl)benzoic acid (**10**) were obtained in nearly quantitative yields (96 and 99%). Then, treatment of acids **9** and **10** with thionyl chloride in a hot toluene medium gave the corresponding chlorides, which were introduced in the acylation reaction with thiazole-2-amine **11** under basic conditions affording amides **12** and **13** in very good yields (79 and 77%). Finally, transformation of these compounds into organoboron complexes **2** and **3** was realized by condensation with boron trifluoride in the presence of *N*,*N*-diisopropylethylamine (DIPEA), giving the final products in 37 and 40% yields, respectively. The chemical structures of the obtained compounds were fully confirmed by ^{1}H, ^{13}C and ^{19}F NMR spectroscopy and high-resolution mass spectrometry (HRMS).

Additionally, the structure of complex **2** was verified by single-crystal X-ray diffraction (Fig. 2, Fig. S1, Tables S1 and S2 in the ESI†). In the solid crystals of the compound, the carbazole moiety is twisted against the phenyl linker plane owing to the intramolecular interactions between the *ortho*-hydrogen atoms of both units. The corresponding dihedral angle (Θ_1) is *ca.* 45.5°. Meanwhile, the position of the oxadiazaboronine ring plane is almost coplanar with the phenyl linker (Θ_2 = 2.1°, Fig. 2a). Complex **2** exhibits molecular packing, characterized by a monoclinic system with four molecules in the unit cell and the $P2_1/c$ space group (Table S1†). In the structure, the neighboring molecules interact by numerous CH···F and CH···O hydrogen bonds, as well as by weak n–π and π–π interactions (Fig. 2c and d), which contributes a weak ACQ effect, thereby leading to the preservation of the emissive properties of the compounds in the solid state.

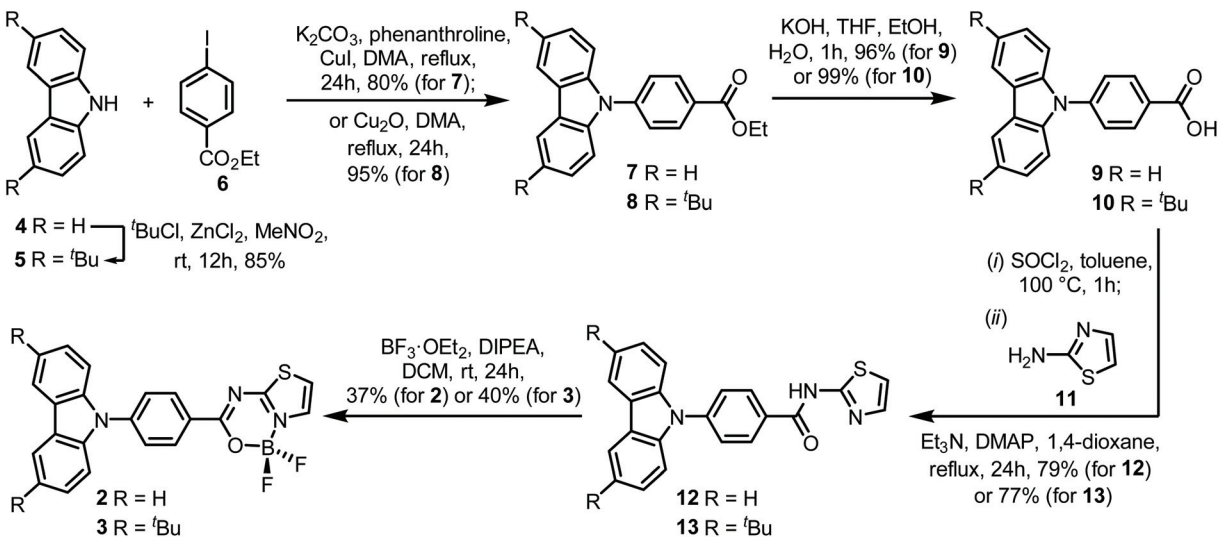

Scheme 1 Synthesis of organoboron complexes **2** and **3**.

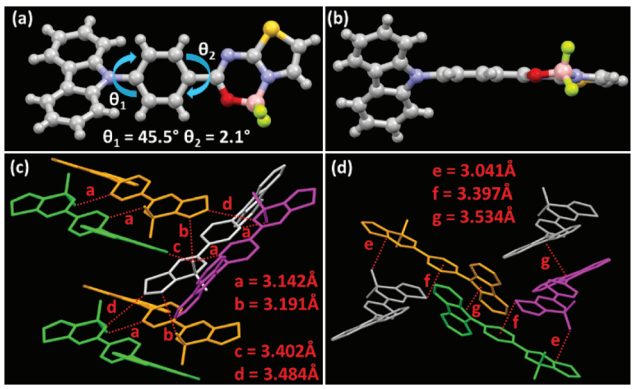

Fig. 2 Single crystal analysis of compound **2**: (a) top and (b) front views; intermolecular interactions: (c) hydrogen bonds and (d) n–π and π–π interactions.

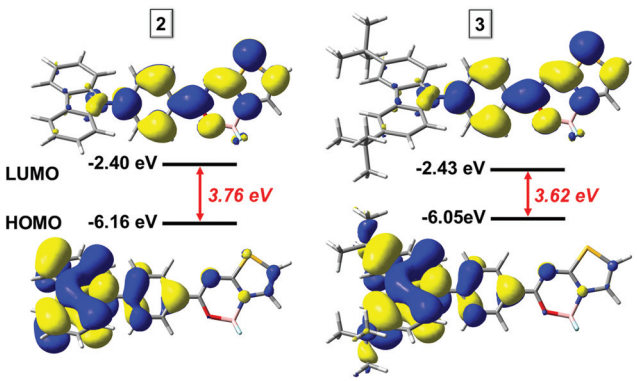

Fig. 3 Frontier molecular orbitals of compounds **2** and **3**.

The thermal properties of complexes **2** and **3** were investigated by differential scanning calorimetry (DSC) and thermogravimetric analysis (TGA). DSC experiments indicated that during the heating scans, compounds **2** and **3** showed single melting peaks at 245 and 315 °C, respectively. Noticeably, no obvious glass transition temperature was observed for these compounds (Fig. S2 in the ESI†). TGA (Fig. S3 in the ESI†) performed under a nitrogen atmosphere showed that organoboron dyes **2** and **3** had high thermal stability with 5% weight loss temperatures (T_d) of 313 and 316 °C, respectively.

Quantum chemical calculations

To predict the electronic properties and molecular geometries of compounds **2** and **3** at the molecular level, density functional theory (DFT) and time-dependent DFT (TD-DFT) calculations at the M06/def2tzvp level of theory were carried out. In the ground state, the lowest-energy conformations of the two compounds have twisted geometry with torsion angles between the carbazole unit and the phenylene linker of *ca.* 47.6 and 48.9° for **2** and **3**, respectively (Fig. S4 in the ESI†). The phenyl linker and the oxadiazaboronine ring are in an almost coplanar position in each molecule. The calculated parameters show good correlation with the X-ray single crystal analysis data obtained for dye **2** (Fig. 2). Consequently, significant HOMO–LUMO separation is observed for both compounds: the HOMOs are mainly located on the carbazole moiety, whereas the LUMOs are dispersed on the planar thiazolo[3,2-*c*]oxadiazaborinine unit and the conjugated phenyl linker ring (Fig. 3).

The calculated energy gap between the HOMO and LUMO of compounds **2** and **3** is 3.76 and 3.62 eV, respectively, inducing the violet light absorption ability. TD-DFT calculations (Table S3 in the ESI†) show that low-lying transition occurs from the HOMO to the LUMO, demonstrating large oscillator strengths ($f \approx 0.69$) for both dyes. These results show that the emission can be attributed to intramolecular charge transfer (ICT).

Photophysical properties in solutions

The photophysical properties of the dilute solutions of organoboron dyes **2** and **3** in five solvents with different polarities (toluene, THF, DCM, acetone, and acetonitrile) were studied by UV-vis absorption and photoluminescence (PL) spectrometries.

The UV-vis absorption spectra of the organoboron complexes were hardly affected by the solvent polarity. In all the investigated solvents, these dyes exhibited low-energy absorption (centred at 370–384 nm for dye **2** and at 387–399 nm for analogue **3**) (Fig. 4 and Table 1). Thus, the experimentally obtained results are in good agreement with the computational data (Fig. S5 and S6 in the ESI†). For comparison,

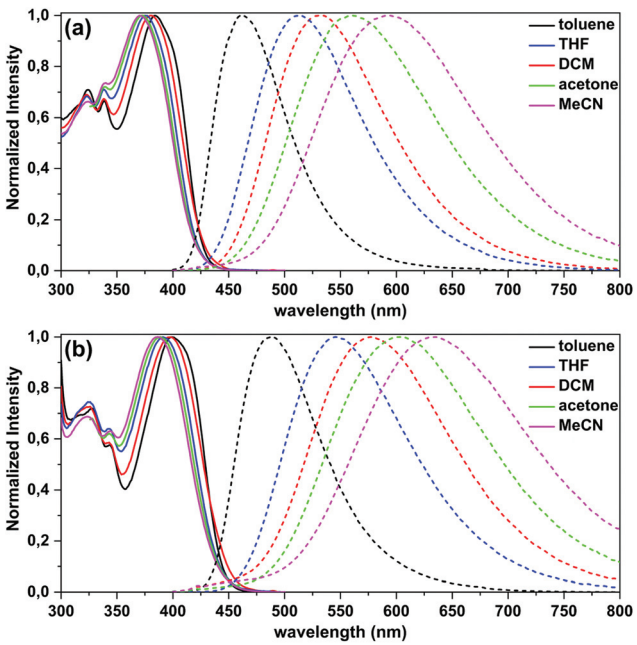

Fig. 4 Normalized absorption (solid lines) and emission (dashed lines) spectra of the solutions of compounds **2** (a) and **3** (b) in toluene (black), THF (blue), DCM (red), acetone (green) and acetonitrile (magenta) (C = 1.0×10^{-5} M; λ_{ex} = 374 nm).

Table 1 Photophysical properties of the solutions of complexes **1**, **2**, and **3** in different solvents

Dye	Solvent	λ_{abs}, nm	ε, M^{-1} cm^{-1}	λ_{em}, nm	$\Delta\upsilon$, cm^{-1}	PLQY
1	Toluene	405	56 600	439	1912	>0.99
	THF	407	54 400	453	2495	0.86
	DCM	402	55 400	454	2849	0.99
	Acetonitrile	402	49 700	469	3553	0.10
2	Toluene	384	23 600	462	4397	0.77
	THF	375	23 300	514	7211	0.57
	DCM	380	21 700	532	7518	0.48
	Acetone	373	23 100	560	8953	0.08
	Acetonitrile	370	20 600	594	10 192	0.02
3	Toluene	399	22 300	489	4613	0.70
	THF	391	25 100	546	7260	0.31
	DCM	398	23 300	578	7895	0.13
	Acetone	389	25 300	605	9178	0.02
	Acetonitrile	387	24 900	631	9992	0.01

compound **1** exhibited an absorption peak maximized at 402–407 nm (Table 1).[14a] The molar absorption coefficient (ε) of the solutions of the dyes ranged from 20 600 to 25 300 M^{-1} cm^{-1}, which is considerably lower than the analogous parameter of previously described analogue **1** (ε = 49 700–56 600 M^{-1} cm^{-1}),[14a] indicating the enhancement of ICT with the structural change of the Me_2N donor group on carbazole or 3,6-di-*tert*-butylcarbazole moieties.

More importantly, the solutions of the investigated dyes exhibited single emission peaks, mirroring the low-energy absorption peaks (Fig. 4). The emission bands displayed bathochromic shifts when the solvent was changed from non-polar toluene (λ_{em} of 462 and 489 nm for compounds **2** and **3**, respectively) to polar acetonitrile (λ_{em} of 594 and 631 nm for dyes **2** and **3**, respectively). Analogically to the absorption spectra, the attachment of ^{t}Bu groups to the carbazole units caused bathochromic shifts of the emission bands, indicating the relatively lower energy level of low-lying singlet excited states. The fluorescence intensity of the solutions of complexes **2** and **3** decreased with the increase of the solvent polarity due to the dissipation of energy with the rotation motions of carbazole and thiazolo[3,2-*c*]oxadiazaborinine moieties. Thereby, in the toluene solution, dyes **2** and **3** exhibit PLQYs of 77 and 70%, respectively. Meanwhile, the emission of acetonitrile solutions is dramatically quenched (PLQY = 1–2%). The solvent polarity-dependent fluorescence quenching is more significant for complex **3** than for analogue **2**. Thus, for THF and DCM solutions of compound **2**, the PLQY is 57 and 48%, respectively, while the values of this parameter for the corresponding solutions of complex **3** are 31 and 13% (Table 1). This observation confirms the enhanced ICT emission of the compound with ^{t}Bu groups attached to the carbazole unit.

The excited-state lifetimes (τ) of the solutions in toluene of dyes **2** and **3** were determined as 3.7 and 4.8 ns, demonstrating the short-lived fluorescence nature of the emission.

Comparison of these emission data with the previously reported data for Me_2N-containing analogue **1** demonstrates that the incorporation of the carbazole donor unit leads to much higher solvatofluorochromic properties and a decrease of the fluorescence quantum yield, especially in the polar medium. These changes could be caused by the increase of the ICT character in the excited state of compounds **2** and **3**.

Solid-state fluorescence properties

The solid-state emissive properties of compounds **2** and **3** were investigated both in crystalline and thin film samples. In the crystalline state, compounds **2** and **3** demonstrated intense emission bands with the maxima at 514 and 496 nm, respectively (Fig. 5 and Table 2), and relatively high quantum yields of 26 and 34%, respectively. The thin film of complex **2** exhibited an almost identical emission spectrum (λ_{em} = 514 nm) to that of the crystalline sample (Fig. 5a). The fluorescence efficiency ($PLQY_{solid}$ = 24%) was also comparable, indicating little change of the fluorescence properties with the change of the morphology. In contrast, the thin film of dye **3** demonstrated bathochromically shifted emission bands (λ_{em} = 521 nm) with respect to those of the crystalline sample. This observation

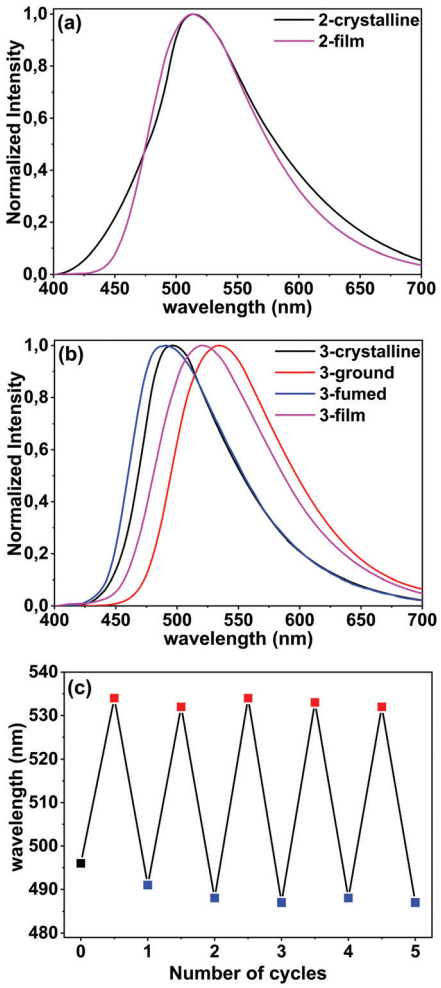

Fig. 5 Normalized emission spectra of dyes **2** (a) and **3** (b) in different solid states (λ_{ex} = 374 nm). Reversible switching of solid-state emission of dye **3** by repeated grinding/DCM-fuming cycles (c).

Table 2 Fluorescence properties of complexes **2** and **3** in the solid state

Comp.	State	λ_{em}, nm	$PLQY_{solid}$	τ, ns	α_1/α_2
2	Crystalline	514	0.26	0.99, 4.28	57.65/42.35
	Film	514	0.24	2.30, 7.42	33.83/66.17
3	Crystalline	496	0.34	1.17, 3.81	60.12/39.88
	Ground	534	0.31	1.46, 6.53	31.17/68.83
	DCM-fumed	491	0.30	0.99, 4.25	65.03/34.97
	Film	521	0.32	2.64, 8.31	57.02/42.98

indicates the morphology-dependent solid-state fluorescence of complex **3**.

In order to shed more light on this phenomenon, we investigated the fluorescence properties of the solid sample after mechanical stimuli. The ground sample of **3** exhibited bluish-green emissions centered at 534 nm, which were even more bathochromically shifted than those of the thin film. Afterwards, DCM-fuming of this sample resulted in hypsochromic shifts of the emission spectra (λ_{em} = 491). The grinding and DCM-fuming procedures were repeated, and the obtained emission spectra were almost identical (Fig. 5c). In comparison, the ground sample of complex **2** demonstrated only a little change in the emission spectrum (λ_{em} = 500 nm) compared with that of the pristine (as-synthesized) crystalline sample (λ_{em} = 514 nm). Moreover, the following DCM-fuming of this ground sample did not have any significant influence on the emissive properties (λ_{em} = 500 nm, Fig. S7 and Table S4 in the ESI†).

The value of the solid-state photoluminescence quantum yield to a great extent depends on interactions between the neighboring molecules in this state. In this context, as was aforementioned (Fig. 2c and d), in the crystalline state, twisted molecules of **2** interacted largely by hydrogen bonds, while the π–π/n–π interactions were weak, contributing a small ACQ effect. In all solid samples of compound **3**, the values of the fluorescence quantum yield were preserved at 30–34%, which were even higher than those for analogue **2**. This phenomenon was apparently caused by the presence of two bulky *tert*-butyl groups in molecules of **3**, which additionally decreased the solid-state π–π/n–π interactions, thus guaranteeing a higher fluorescence efficiency.

The lifetimes of the excited state of the investigated solid samples established from double exponential fits of photoluminescence decay curves were in the range of 0.99–8.31 ns (Table 2). These values were comparative with the corresponding values established for the solutions.

Aggregation-induced emission (AIE) properties

Organoboron complexes **2** and **3** demonstrated good solubility in common organic solvents, such as toluene, tetrahydrofuran, chloroform, dichloromethane, acetone and acetonitrile, but were not soluble in water. On the other hand, as aforementioned, they exhibited low photoluminescence quantum yields in polar solvents (acetone and acetonitrile), and comparatively high quantum yields in the solid state. These data indicate that the investigated compounds should demonstrate AIE ability.

To verify this presumption, we studied the emission properties of equimolar solutions of the complexes in THF/water mixtures with various water fractions (f_w) from 0 to 95% (Fig. 6). In the cases of both compounds, the initial growth of f_w resulted in the decrease of the emission intensity due to the increase of the polarity of the media. However, for dye **2**, when f_w exceeded 80%, a significant increase of the emission intensity was observed (Fig. 6a and c). This observation indicates that solute molecules form nanoscopic aggregates (nanoparticles) in water-dominant dispersions due to their hydrophobic effect. Indeed, the dynamic light scattering (DLS) experiments confirmed the formation of nanoaggregates in the dispersions with an average size of 79 nm (Fig. 6e).

Complex **3** demonstrated even enhanced AIE activity. In this case, the emission intensity was boosted dramatically when f_w exceeded 70%, and was more than 25-fold enhanced for the dispersion containing 95% of water (Fig. 6b and d). DLS measurements showed the formation of nanoaggregates of dye **3** under such conditions with an average size of 89 nm (Fig. 6f).

Conclusions

In conclusion, we developed an efficient synthesis of two new highly thermally stable carbazole-modified thiazolo[3,2-*c*][1,3,5,2]oxadiazaborinines **2** and **3**. The incorporation of a carbazole donor unit into the structure of such organoboron complexes leads to much higher solvatofluorochromism and larger decrease of the fluorescence quantum yield in polar solutions. Complex **3** with two *tert*-butyl substituents at the positions C-3 and C-6 of the carbazole moiety demonstrated morphology-dependent solid-state fluorescence and significant mechanofluorochromic properties ($\Delta\lambda_{em}$ = 43 nm), probably owing to the decrease of n–π/π–π-stacking interactions. Both dyes **2** and **3** demonstrated aggregation-induced emission enhancement. Taken together, through this work, new insights are shown for the preferred design strategies for prospective AIE-active organoboron emitters.

Experimental

General

Chemicals and solvents were obtained from commercial sources (TCI, Acros Organics, FluoroChem, or Aldrich) and were used without further purification. Column chromatography was carried out using silica gel (Merck, 230–400 mesh) as the stationary phase. The NMR spectra were recorded on Bruker Avance II 400 MHz (at 400 and 100 MHz for ^{1}H and ^{13}C NMR spectra, respectively) and Varian VNMRS 500 MHz (at 500, 125 and 470 MHz for ^{1}H, ^{13}C and ^{19}F NMR spectra, respectively) spectrometers for solutions in $CDCl_3$ or DMSO-d_6, referenced to tetramethylsilane or solvent peaks. NMR data

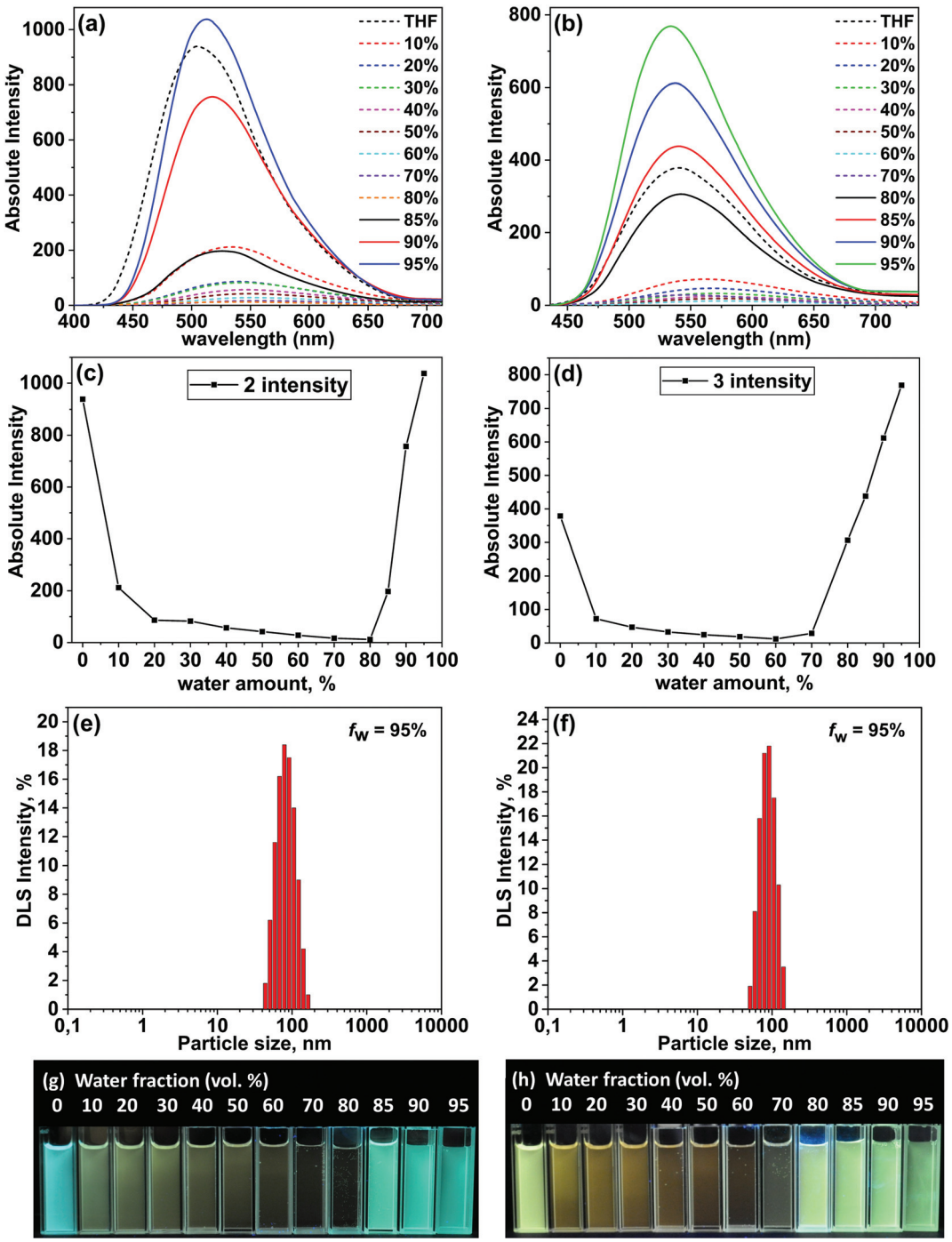

Fig. 6 Emission spectra of the dispersions of dyes **2** (a) and **3** (b) in THF/water mixtures (C = 1.0 × 10^{-5} M; λ_{ex} = 374 nm). Plots of the absorption intensity of **2** (c) and **3** (d) *versus* f_w. Size distribution of complexes **2** (e) and **3** (f) in THF/water medium with water fractions from 0 to 95%. Photographs of the dispersions of **2** (g) and **3** (h) in THF/water mixtures under UV irradiation at 365 nm.

were analysed using Mnova software. Mass spectra were acquired with a Synapt G2-S HDMS (Waters Inc.) mass spectrometer equipped with an electrospray ion source and a quadrupole time-of-flight type mass analyser. The melting points of the synthesized compounds were determined using an Automatic Melting Point System (OptiMelt, Stanford Research Systems). DSC measurements were performed on a DSC Q 100 TA Instrument at a heating rate of 10 °C min^{-1} under a nitrogen atmosphere. TGA was performed on a Metter TGA/SDTA851e/LF/1100 apparatus at a heating rate of 10 °C min^{-1} under a nitrogen atmosphere.

Single crystals of organoboron complex **2** were obtained by slow evaporation of its solution in hexanes/DCM (1 : 1) at room temperature. X-ray intensity data were collected at 100 K on a

SuperNova Agilent diffractometer using Cu Kα (λ = 1.54184 Å) radiation. Data reduction was processed using CrysAlisPro (Agilent Technologies, Version 1.171.35.21b). The structures were solved by direct methods and refined using SHELXL Software Package.[16] DFT and TD-DFT calculations were performed using Gaussian 09 software[17] with the inclusion of the DCM solvent effect through the conductor-like polarizable continuum model (CPCM). UV–vis absorption spectra were recorded on a PerkinElmer Lambda 35 spectrometer for *ca.* 1.0 × 10^{-5} M solutions of dyes. Fluorescence spectra were recorded using an Edinburgh Instruments FLS980 fluorescence spectrometer (λ_{ex} = 374 nm) for both *ca.* 1.0 × 10^{-5} M solutions and solid crystals of the investigated dyes. Absolute photoluminescence quantum yields of the samples were measured on the same machine using a calibrated integrating sphere. Fluorescence decays of the solutions and of the solid-state samples were recorded with a PicoQuant PDL 820 ps pulsed diode laser as an excitation source (λ_{ex} = 374 nm) using a time-correlated single-photon counting technique. DLS was measured using a Malvern Zetasizer.

The THF/water mixtures of various ratios were prepared by slowly adding distilled water into solutions of dye **2** or **3** in THF under sonication, while the concentration was maintained at 1.0 × 10^{-5} M. The emission spectra and DLS of the obtained mixture were measured immediately.

Synthesis

3,6-Di-*tert*-butyl-9*H*-carbazole (5). This compound was obtained using a modified literature procedure.[15] The reaction was conducted under an argon atmosphere. *tert*-Butyl chloride (8.40 mL, 76.25 mmol) was added to a solution of carbazole (**4**, 5.00 g, 29.90 mmol) and zinc chloride (10.19 g, 74.75 mmol) in nitromethane (40 mL). The solution was stirred at room temperature for 12 h. After that, water (50 mL) was added and the mixture was extracted with dichloromethane (3 × 60 mL). The combined organic layer was washed with water (50 mL), saturated sodium carbonate solution (30 mL), and brine (30 mL), dried over anhydrous Na_2SO_4, filtered and concentrated. The obtained solid was purified by column chromatography on silica gel (hexanes/ethyl acetate = 100 : 0 to 99 : 1, v/v) to give product **5** in 85% (7.14 g) yield. Mp. 225.3–227.4 °C, white powder. ^{1}H NMR (400 MHz, $CDCl_3$): δ = 8.11 (2H, d, J = 1.9 Hz, Ar–H), 7.78 (1H, br s, N–H), 7.49 (2H, dd, J = 8.6 Hz, J = 1.9 Hz, Ar–H), 7.32 (2H, d, J = 8.6 Hz, Ar–H), 1.48 [18H, s, 2 × $C(CH_3)_3$] ppm; ^{13}C NMR (100 MHz, $CDCl_3$): δ = 142.2 (2C), 138.0 (2C), 123.5 (2C), 123.3 (2C), 116.2 (2C), 110.0 (2C), 34.7 (C2), 32.0 (6C) ppm. HRMS (ESI-TOF) calcd for $C_{20}H_{26}N$ $[M + H]^+$: 280.2065, found: 280.2056.

Ethyl 4-(9*H*-carbazol-9-yl)benzoate (7). This compound was obtained using a modified literature procedure.[18] A mixture of carbazole (**4**, 1.00 g, 5.98 mmol), ethyl 4-iodobenzoate (**6**, 1.00 mL, 5.98 mmol), copper(I) iodide (114 mg, 0.60 mmol), potassium carbonate (2.46 g, 17.94 mmol) and 1,10-phenanthroline (108 mg, 0.60 mmol) in dimethylacetamide (10 mL) was refluxed under argon for 24 h. After cooling, a saturated aqueous solution of ammonium chloride (15 mL) was added and the mixture was extracted with DCM (3 × 20 mL). The organic phases were washed with water (2 × 15 mL) and a saturated aqueous solution of ammonium chloride (2 × 15 mL), dried over Na_2SO_4, and concentrated. The residue was separated by column chromatography on silica gel (hexanes, next hexanes/AcOEt = 99 : 1) to afford a pure product **7** in 80% (1.45 g) yield. Mp. 97.3–98.8 °C (lit.[18] 94–95 °C), yellowish powder. ^{1}H NMR (500 MHz, $CDCl_3$): δ = 8.30 (2H, d, J = 8.5 Hz, Ar–H), 8.15 (2H, br d, J = 7.7 Hz, Ar–H), 7.69 (2H, d, J = 8.5 Hz, Ar–H), 7.48 (2H, br d, J = 7.8 Hz, Ar–H), 7.43 (2H, ddd, J = 8.0 Hz, J = 7.7 Hz, J = 1.2 Hz, Ar–H), 7.32 (2H, ddd, J = 8.0 Hz, J = 7.8 Hz, J = 1.2 Hz, Ar–H), 4.46 (2H, d, J = 7.1 Hz, CH_2), 1.46 (3H, t, J = 7.1 Hz, CH_3) ppm; ^{13}C NMR (125 MHz, $CDCl_3$): δ = 165.9, 141.9, 140.3 (2C), 131.3 (2C), 129.0, 126.4 (2C), 126.1 (2C), 123.8 (2C), 120.5 (2C), 120.4 (2C), 109.7 (2C), 61.2, 14.4 ppm. HRMS (ESI-TOF) calcd for $C_{21}H_{17}NO_2$ $[M]^+$: 315.1259, found: 315.1254.

Ethyl 4-(3,6-di-*tert*-butyl-9*H*-carbazol-9-yl)benzoate (8). This compound was obtained using a modified literature procedure.[19] A mixture of 3,6-di-*tert*-butylcarbazole (**5**, 1.50 g, 5.37 mmol), ethyl 4-iodobenzoate (**6**, 1.00 mL, 5.98 mmol) and copper(I) oxide (1.61 g, 11.27 mmol) in dimethylacetamide (10 mL) was refluxed for 24 h under argon. After cooling, a saturated aqueous solution of ammonium chloride (15 mL) was added and the mixture was extracted with DCM (3 × 20 mL). The organic phases were washed with water (2 × 15 mL) and a saturated aqueous solution of ammonium chloride (2 × 15 mL), dried over Na_2SO_4, and concentrated. The residue was separated by column chromatography on silica gel (hexanes, next hexanes/AcOEt = 99 : 1) to afford a pure product **8** in 95% (2.19 g) yield. Mp. 180.9–182.0 °C, white powder. ^{1}H NMR (400 MHz, $CDCl_3$): δ = 8.28 (2H, d, J = 8.6 Hz, Ar–H), 8.16 (2H, d, J = 1.8 Hz, Ar–H), 7.68 (2H, d, J = 8.6 Hz, Ar–H), 7.49 (2H, dd, J = 8.7 Hz, J = 1.8 Hz, Ar–H), 7.43 (2H, d, J = 8.7 Hz, Ar–H), 4.47 (2H, d, J = 7.1 Hz, CH_2), 1.49 [18H, s, 2 × $C(CH_3)_3$], 1.47 (3H, t, J = 7.1 Hz, CH_3) ppm; ^{13}C NMR (100 MHz, $CDCl_3$): δ = 166.0, 143.5 (2C), 142.5, 138.6 (2C), 131.2 (2C), 128.5, 125.8 (2C), 123.8 (2C), 123.8 (2C), 116.4 (2C), 109.2 (2C), 61.1, 34.7 (C2), 32.0 (6C), 14.4 ppm. HRMS (ESI-TOF) calcd for $C_{29}H_{34}NO_2$ $[M + H]^+$: 428.2590, found: 428.2587.

4-(9*H*-Carbazol-9-yl)benzoic acid (9). A mixture of ester **7** (1.20 g, 3.80 mmol), THF (20 mL), EtOH (4 mL), H_2O (4 mL) and KOH (0.64 g, 11.42 mmol) was refluxed for 1 h. After cooling, the solvents were evaporated and water (5 mL) and 5 N HCl solution were added to adjust the pH to ~5. The mixture was left in a fridge for 4 h. The precipitate was filtered, washed with water, and dried to give product **9** in 96% (1.05 g) yield. Mp. 256.8–259.6 °C, white powder. ^{1}H NMR (500 MHz, DMSO-d_6): δ = 8.21–8.27 (4H, m, Ar–H), 7.77 (2H, d, J = 8.4 Hz, Ar–H), 7.48 (2H, d, J = 8.1 Hz, Ar–H), 7.44 (2H, dd, J = 8.1 Hz, J = 7.1 Hz, Ar–H), 7.31 (2H, dd, J = 7.5 Hz, J = 7.1 Hz, Ar–H) ppm; ^{13}C NMR (125 MHz, DMSO-d_6): δ = 166.7, 140.9, 139.6 (2C), 131.3 (2C), 129.4, 126.4 (2C), 126.3 (2C), 123.1 (2C), 120.6 (2C), 120.6 (2C), 109.8 (2C) ppm. HRMS (ESI-TOF) calcd for $C_{19}H_{12}NO_2$ $[M - H]^-$: 286.0868, found: 286.0861.

4-(3,6-Di-*tert*-butyl-9*H*-carbazol-9-yl)benzoic acid (10). A mixture of ester **8** (1.30 g, 3.04 mmol), THF (25 mL), EtOH (5 mL), H_2O (5 mL) and KOH (0.51 g, 9.12 mmol) was refluxed for 1 h. After cooling, the solvents were evaporated and water (5 mL) and 5 N HCl solution were added to adjust the pH to ~5. The mixture was left in a fridge for 4 h. The precipitate was filtered, washed with water, and dried to give product **10** in 99% (1.20 g) yield. Mp. 273.5–276.8 °C, white powder. ^{1}H NMR (600 MHz, DMSO-d_6): δ = 8.30 (2H, br s, Ar–H), 8.19 (2H, d, J = 8.0 Hz, Ar–H), 7.71 (2H, d, J = 8.0 Hz, Ar–H), 7.48 (2H, d, J = 8.6 Hz, Ar–H), 7.40 (2H, d, J = 8.6 Hz, Ar–H), 1.41 [18H, s, 2 × $C(CH_3)_3$] ppm; ^{13}C NMR (150 MHz, DMSO-d_6): δ = 167.1, 143.0 (2C), 140.7, 138.1 (2C), 131.1 (2C), 131.0, 125.5 (2C), 123.8 (2C), 123.2 (2C), 116.8 (2C), 109.2 (2C), 34.5 (2C), 31.8 (6C) ppm. HRMS (ESI-TOF) calcd for $C_{27}H_{28}NO_2$ $[M - H]^-$: 398.2120, found: 398.2108.

4-(9*H*-Carbazol-9-yl)-*N*-(thiazol-2-yl)benzamide (12). Thionyl chloride (142 μL, 1.95 mmol, 1.5 equiv.) was added to a suspension of acid **9** (374 mg, 1.30 mmol, 1.0 equiv.) in dry toluene (20 mL). The reaction mixture was heated at 100 °C for 1 h. After cooling, the solvent and the rest of $SOCl_2$ were evaporated under vacuum. The obtained benzoyl chloride was dissolved in 1,4-dioxane (20 mL); amine **11** (196 mg, 1.95 mmol, 1.5 equiv.), dry triethylamine (545 μL, 3.91 mmol, 3.0 equiv.) and DMAP (8 mg, 0.07 mmol, 0.05 equiv.) were added. Next, the reaction mixture was refluxed for 24 h. Water (30 mL) and a saturated aqueous solution of $NaHCO_3$ (30 mL) were added and the mixture was extracted with DCM (3 × 50 mL). The combined organic layers were dried over anhydrous Na_2SO_4, filtered and concentrated. The crude product was purified by column chromatography on silica gel (hexanes/dichloromethane from 4 : 1 to 0 : 1, v/v) to afford pure amide **12** in 79% (380 g) yield. Mp. 286.0–287.2 °C. ^{1}H NMR (500 MHz, DMSO-d_6): δ = 12.82 (1H, br s, N–H), 8.41 (2H, d, J = 8.5 Hz, Ar–H), 8.27 (2H, d, J = 7.7 Hz, Ar–H), 7.83 (2H, d, J = 8.5 Hz, Ar–H), 7.60 (1H, d, J = 3.6 Hz, thiazole–H), 7.44–7.52 (4H, m, Ar–H), 7.29–7.36 (3H, m, Ar–H, thiazole–H) ppm; ^{13}C NMR (125 MHz, DMSO-d_6): δ = 164.4, 158.9, 140.6, 139.6 (2C), 137.5, 130.8, 130.2 (2C), 126.5 (2C), 126.3 (2C), 123.1 (2C), 120.6 (2C), 120.6 (2C), 113.9, 109.8 (2C) ppm. HRMS (ESI-TOF) calcd for $C_{22}H_{15}N_3OSNa$ $[M + Na]^+$: 392.0834, found: 392.0827.

4-(3,6-Di-*tert*-butyl-9*H*-carbazol-9-yl)-*N*-(thiazol-2-yl)benzamide (13). Thionyl chloride (131 μL, 1.80 mmol, 1.5 equiv.) was added to a suspension of acid **10** (480 mg, 1.20 mmol, 1.0 equiv.) in dry toluene (20 mL). The reaction mixture was heated at 100 °C for 1 h. After cooling, the solvent and the rest of $SOCl_2$ were evaporated under vacuum. The obtained benzoyl chloride was dissolved in 1,4-dioxane (20 mL); amine **11** (180 mg, 1.80 mmol, 1.5 equiv.), dry triethylamine (503 μL, 3.60 mmol, 3.0 equiv.) and DMAP (7 mg, 0.06 mmol, 0.05 equiv.) were added. Next, the reaction mixture was refluxed for 24 h. Water (30 mL) and a saturated aqueous solution of $NaHCO_3$ (30 mL) were added and the mixture was extracted with DCM (3 × 50 mL). The combined organic layers were dried over anhydrous Na_2SO_4, filtered and concentrated. The crude product was purified by column chromatography on silica gel (hexanes/dichloromethane from 4 : 1 to 0 : 1, v/v) to afford pure amide **13** in 77% (446 g) yield. Mp. 327.6–330.5 °C. ^{1}H NMR (500 MHz, $CDCl_3$): δ = 11.24 (1H, br s, N–H), 8.23 (2H, d, J = 8.5 Hz, Ar–H), 8.15 (2H, d, J = 1.9 Hz, Ar–H), 7.78 (2H, d, J = 8.5 Hz, Ar–H), 7.50 (2H, dd, J = 8.6 Hz, J = 1.9 Hz, Ar–H), 7.46 (2H, d, J = 8.6 Hz, Ar–H), 7.35 (1H, d, J = 3.6 Hz, thiazole–H), 7.05 (1H, d, J = 3.6 Hz, thiazole–H), 1.48 [18H, s, 2 × $C(CH_3)_3$] ppm; ^{13}C NMR (125 MHz, $CDCl_3$): δ = 164.3, 159.4, 143.8 (2C), 142.6, 138.5 (2C), 137.4, 130.0, 129.5 (2C), 126.3 (2C), 124.0 (2C), 123.9 (2C), 116.5 (2C), 114.0, 109.2 (2C), 34.8 (2C), 32.0 (6C) ppm. HRMS (ESI-TOF) calcd for $C_{30}H_{31}N_3OSNa$ $[M + Na]^+$: 504.2086, found: 504.2087.

3-(4-(9*H*-Carbazol-9-yl)phenyl)-1,1-difluoro-1*H*-1λ^4,8λ^4-thiazolo[3,2-*c*][1,3,5,2]oxadiazaborinine (2). Distilled *N*,*N*-diisopropylethylamine (2.64 mL, 15.16 mmol, 20 equiv.) and $BF_3{\cdot}Et_2O$ (0.94 mL, 7.67 mmol, 10 equiv.) were added to a solution of amide **12** (280 mg, 0.76 mmol, 1 equiv.) in dry DCM (30 mL) under an argon atmosphere. The reaction mixture was stirred for 24 h at room temperature and then washed with water. The organic phase was dried over anhydrous Na_2SO_4 and filtered. The solvent was removed under reduced pressure, and the crude product was purified by column chromatography (hexanes/dichloromethane from 8 : 1 to 1 : 1, v/v) to obtain pure product **2** in 37% yield (117 mg). Mp. 244.7–246.8 °C. ^{1}H NMR (500 MHz, $CDCl_3$): δ = 8.58 (2H, d, J = 8.6 Hz, Ar–H), 8.15 (2H, d, J = 8.0 Hz, Ar–H), 7.76 (2H, d, J = 8.6 Hz, Ar–H), 7.64 (1H, d, J = 4.3 Hz, thiazole–H), 7.52 (2H, d, J = 8.0 Hz, Ar–H), 7.45 (2H, ddd, J = 8.0 Hz, J = 7.6 Hz, J = 1.3 Hz, Ar–H), 7.33 (2H, ddd, J = 8.0 Hz, J = 7.6 Hz, J = 1.0 Hz, Ar–H), 7.19 (1H, d, J = 4.3 Hz, thiazole–H) ppm; ^{13}C NMR (125 MHz, $CDCl_3$): δ = 173.4, 165.9, 143.0, 140.1 (2C), 131.8 (2C), 130.3, 129.5, 126.3 (2C), 126.3 (2C), 124.0 (2C), 120.7 (2C), 120.5 (2C), 114.7, 109.9 (2C) ppm; ^{19}F NMR (470 MHz, $CDCl_3$): δ = −135.18 (2F, m, BF_2) ppm. HRMS (ESI-TOF) calcd for $C_{22}H_{15}BN_3OF_2S$ $[M + H]^+$: 418.0997, found: 418.0995.

3-(4-(3,6-Di-*tert*-butyl-9*H*-carbazol-9-yl)phenyl)-1,1-difluoro-1*H*-1λ^4,8λ^4-thiazolo[3,2-*c*][1,3,5,2]oxadiazaborinine (3). Distilled *N*,*N*-diisopropylethylamine (2.24 mL, 12.87 mmol, 20 equiv.) and $BF_3{\cdot}Et_2O$ (0.79 mL, 6.43 mmol, 10 equiv.) were added to a solution of amide **13** (310 mg, 0.64 mmol, 1 equiv.) in dry DCM (30 mL) under an argon atmosphere. The reaction mixture was stirred for 24 h at room temperature and then washed with water. The organic phase was dried over anhydrous Na_2SO_4 and filtered. The solvent was removed under reduced pressure, and the crude product was purified by column chromatography (hexanes/dichloromethane from 8 : 1 to 1 : 1, v/v) to obtain pure product **3** in 40% yield (138 mg). Mp. 313.1–315.2 °C. ^{1}H NMR (500 MHz, $CDCl_3$): δ = 8.55 (2H, d, J = 8.6 Hz, Ar–H), 8.14 (2H, br s, Ar–H), 7.74 (2H, d, J = 8.6 Hz, Ar–H), 7.63 (1H, d, J = 4.3 Hz, thiazole–H), 7.45–7.51 (4H, m, Ar–H), 7.18 (1H, d, J = 4.3 Hz, thiazole–H), 1.47 [18H, s, 2 × $C(CH_3)_3$] ppm; ^{13}C NMR (125 MHz, $CDCl_3$): δ = 173.5, 166.0, 143.8 (2C), 143.6, 138.4 (2C), 131.8 (2C), 130.2, 128.8, 125.7 (2C), 124.0 (2C), 123.9 (2C), 116.4 (2C), 114.6, 109.4 (2C), 34.8 (2C), 32.0 (6C) ppm; ^{19}F NMR (470 MHz, $CDCl_3$): δ = −135.27 (2F, m, BF_2) ppm. HRMS (ESI-TOF) calcd for $C_{30}H_{31}BN_3OF_2S$ $[M + H]^+$: 530.2249, found: 530.2258.

Conflicts of interest

There are no conflicts to declare.

Acknowledgements

This work was supported by Poland's National Science Centre (Grant No. UMO-2019/03/X/ST4/00037). The calculation research was supported by PLGrid Infrastructure. Jurate Simokaitiene is gratefully acknowledged for the help with the DSC and TGA measurements.

Notes and references

1 (*a*) Y. Hong, J. W. Y. Lam and B. Z. Tang, *Chem. Soc. Rev.*, 2011, **40**, 5361–5388; (*b*) J. Mei, N. L. C. Leung, R. T. K. Kwok, J. W. Y. Lam and B. Z. Tang, *Chem. Rev.*, 2015, **115**, 11718–11940; (*c*) K. Kokado and K. Sada, *Angew. Chem., Int. Ed.*, 2019, **58**, 8632–8639; (*d*) Z. Zhao, H. Zhang, J. W. Y. Lam and B. Z. Tang, *Angew. Chem., Int. Ed.*, 2020, **59**, 9888–9907; (*e*) S. Suzuki, S. Sasaki, A. S. Sairi, R. Iwai, B. Z. Tang and G. Konishi, *Angew. Chem., Int. Ed.*, 2020, **59**, 9856–9867; (*f*) F. Wgrthner, *Angew. Chem., Int. Ed.*, 2020, **59**, 14192–14196.

2 (*a*) H. Chen, S. Li, M. Wu, Kenry, Z. Huang, C.-S. Lee and B. Liu, *Angew. Chem., Int. Ed.*, 2020, **59**, 632–636; (*b*) D. Wang, M. M. S. Lee, W. Xu, G. Shan, X. Zheng, R. T. K. Kwok, J. W. Y. Lam, X. Hu and B. Z. Tang, *Angew. Chem., Int. Ed.*, 2019, **58**, 5628–5632; (*c*) W. Xu, M. M. S. Lee, J.-J. Nie, Z. Zhang, R. T. K. Kwok, J. W. Y. Lam, F.-J. Xu, D. Wang and B. Z. Tang, *Angew. Chem., Int. Ed.*, 2020, **59**, 9610–9616; (*d*) J. Wang, X. Zhu, J. Zhang, H. Wang, G. Liu, Y. Bu, J. Yu, Y. Tian and H. Zhou, *ACS Appl. Mater. Interfaces*, 2020, **12**, 1988–1996; (*e*) L. Zhang, W. Che, Z. Yang, X. Liu, S. Liu, Z. Xie, D. Zhu, Z. Su, B. Z. Tang and M. R. Bryce, *Chem. Sci.*, 2020, **11**, 2369–2374.

3 (*a*) N. Zhao, C. Ma, W. Yang, W. Yin, J. Wei and N. Li, *Chem. Commun.*, 2019, **55**, 8494–8497; (*b*) F. Hu, G. Qi, Kenry, D. Mao, S. Zhou, M. Wu, W. Wu and B. Liu, *Angew. Chem., Int. Ed.*, 2020, **59**, 9288–9292; (*c*) X. Zhao, Z. Fan, Y. Qiao, Y. Chen, S. Wang, X. Yue, T. Shen, W. Liu, J. Yang, H. Gao, X. Zhan, L. Shang, Y. Yin, W. Zhao, D. Ding, R. Xi and M. Meng, *ACS Appl. Mater. Interfaces*, 2020, **12**, 16114–16124; (*d*) W. Qin, N. Alifu, J. W. Y. Lam, Y. Cui, H. Su, G. Liang, J. Qian and B. Z. Tang, *Adv. Mater.*, 2020, **32**, 2000364; (*e*) R. Matsubara, T. Kaiba, A. Nakata, T. Yabuta, M. Hayashi, M. Tsubaki, T. Uchino and E. Chatani, *J. Org. Chem.*, 2019, **84**, 5535–5547.

4 (*a*) B. Huang, W.-C. Chen, Z. Li, J. Zhang, W. Zhao, Y. Feng, B. Z. Tang and C.-S. Lee, *Angew. Chem., Int. Ed.*, 2018, **57**, 12473–12477; (*b*) H. Nie, B. Chen, J. Zeng, Y. Xiong, Z. Zhao and B. Z. Tang, *J. Mater. Chem. C*, 2018, **6**, 3690–3698; (*c*) S. Y. Park, S. Choi, G. E. Park, H. J. Kim, C. Lee, J. S. Moon, S. W. Kim, S. Park, J. H. Kwon, M. J. Cho and D. H. Choi, *ACS Appl. Mater. Interfaces*, 2018, **10**, 14966–14977; (*d*) F. Ma, G. Zhao, Y. Zheng, F. He, K. Hasrat and Z. Qi, *ACS Appl. Mater. Interfaces*, 2020, **12**, 1179–1189; (*e*) Z. Qiu, Z. Yang, W.-C. Chen, L. Xing, S. Hu, S. Ji, Q. Yang, N. Cai, X. Ouyang and Y. Huo, *J. Mater. Chem. C*, 2020, **8**, 4139–4147; (*f*) W. Feng, Q. Su, Y. Ma, Z. Džolić, F. Huang, Z. Wang, S. Chen and B. Z. Tang, *J. Org. Chem.*, 2020, **85**, 158–167.

5 L. K. Hiscock, B. M. Raycraft, M. Wałęsa-Chorab, C. Cambe, A. Malinge, W. G. Skene, H. Taing, S. H. Eichhorn, L. N. Dawe and K. E. Maly, *Chem. – Eur. J.*, 2019, **25**, 1018–1028.

6 (*a*) R. Arumugaperumal, P. Raghunath, M.-C. Lin and W.-S. Chung, *Chem. Mater.*, 2018, **30**, 7221–7233; (*b*) D. Dai, Z. Li, J. Yang, C. Wang, J.-R. Wu, Y. Wang, D. Zhang and Y.-W. Yang, *J. Am. Chem. Soc.*, 2019, **141**, 4756–4763; (*c*) Y. Huang, J. Ji, J. Zhang, F. Wang and J. Lei, *Chem. Commun.*, 2020, **56**, 313–316.

7 J.-Y. Chen, G. Kadam, A. Gupta, Anuradha, S. V. Bhosale, F. Zheng, C.-H. Zhou, B.-H. Jia, D. S. Dalal and J.-L. Li, *Chem. – Eur. J.*, 2018, **24**, 14668–14678.

8 (*a*) M. Donnier-Maréchal, S. Abdullayev, M. Bauduin, Y. Pascal, M.-Q. Fu, X.-P. He, E. Gillon, A. Imberty, E. Kipnis, R. Dessein and S. Vidal, *Org. Biomol. Chem.*, 2018, **16**, 8804–8809; (*b*) B. Sadowski, K. Hassanein, B. Ventura and D. T. Gryko, *Org. Lett.*, 2018, **20**, 3183–3186; (*c*) W. Chen, C. Zhang, X. Han, S. H. Liu, Y. Tan and J. Yin, *J. Org. Chem.*, 2019, **84**, 14498–14507; (*d*) N. Adarsh and A. S. Klymchenko, *Nanoscale*, 2019, **11**, 13977–13987.

9 (*a*) L. Zhou, D. Xu, H. Gao, A. Han, Y. Yang, C. Zhang, X. Liu and F. Zhao, *RSC Adv.*, 2016, **6**, 69560–69568; (*b*) H. Gao, Y. Gao, C. Wang, D. Hu, Z. Xie, L. Liu, B. Yang and Y. Ma, *ACS Appl. Mater. Interfaces*, 2018, **10**, 14956–14965; (*c*) X.-R. Jia, H.-J. Yu, J. Chen, W.-J. Gao, J.-K. Fang, Y.-S. Qin, X.-K. Hu and G. Shao, *Chem. – Eur. J.*, 2018, **24**, 19053–19059; (*d*) D. Wang, H. Su, R. T. K. Kwok, X. Hu, H. Zou, Q. Luo, M. M. S. Lee, W. Xu, J. W. Y. Lam and B. Z. Tang, *Chem. Sci.*, 2018, **9**, 3685–3693; (*e*) W. Chen, S. Zhang, G. Dai, Y. Chen, M. Li, X. Zhao, Y. Chen and L. Chen, *Chem. – Eur. J.*, 2019, **25**, 469–473.

10 G. Grybauskaite-Kaminskiene, D. Volyniuk, V. Mimaite, O. Bezvikonnyi, A. Bucinskas, G. Bagdziunas and J. V. Grazulevicius, *Chem. – Eur. J.*, 2018, **24**, 9581–9591.

11 (*a*) A. Loudet and K. Burgess, *Chem. Rev.*, 2007, **107**, 4891–4932; (*b*) G. Ulrich, R. Ziessel and A. Harriman, *Angew. Chem., Int. Ed.*, 2008, **47**, 1184–1201; (*c*) T. Kowada, H. Maeda and K. Kikuchi, *Chem. Soc. Rev.*, 2015, **44**, 4953–4972; (*d*) J. Wang, N. Boens, L. Jiao and E. Hao, *Org. Biomol. Chem.*, 2020, **18**, 4135–4156; (*e*) D. Frath, J. Massue, G. Ulrich and R. Ziessel, *Angew. Chem., Int. Ed.*, 2014, **53**, 2290–2310.

12 Z. Liu, Z. Jiang, M. Yan and X. Wang, *Front. Chem.*, 2019, **7**, 712.

13 (*a*) Y. Wu, Z. Li, Q. Liu, X. Wang, H. Yan, S. Gong, Z. Liu and W. He, *Org. Biomol. Chem.*, 2015, **13**, 5775–5782; (*b*) F. Qi, J. Lin, X. Wang, P. Cui, H. Yan, S. Gong, C. Ma, Z. Liu and W. Huang, *Dalton Trans.*, 2016, **45**, 7278–7284; (*c*) D. Frath, K. Benelhadj, M. Munch, J. Massue and

G. Ulrich, *J. Org. Chem.*, 2016, **81**, 9658–9668; (*d*) P. Zhang, W. Liu, G. Niu, H. Xiao, M. Wang, J. Ge, J. Wu, H. Zhang, Y. Li and P. Wang, *J. Org. Chem.*, 2017, **82**, 3456–3462; (*e*) W. Duan, Q. Liu, Y. Huo, J. Cui, S. Gong and Z. Liu, *Org. Biomol. Chem.*, 2018, **16**, 4977–4984; (*f*) F. Qiu, N. Zhang, R. Tang, M. Zhou, Y. Wang, W. Wei, S. Bi, S. Han and F. Zhang, *J. Org. Chem.*, 2018, **83**, 12977–12984; (*g*) H. Gao, D. Xu, Y. Wang, C. Zhang, Y. Yang, X. Liu, A. Han and Y. Wang, *Dyes Pigm.*, 2018, **150**, 165–173; (*h*) X. Yan, P. Zhu, Z. Zhou, H. Yang, H. Lan and S. Xiao, *RSC Adv.*, 2019, **9**, 35872–35877; (*i*) K. I. Lugovik, A. K. Eltyshev, P. O. Suntsova, P. A. Slepukhin, E. Benassi and N. P. Belskaya, *Chem. – Asian J.*, 2018, **13**, 311–324.

14 (*a*) M. A. Potopnyk, R. Lytvyn, Y. Danyliv, M. Ceborska, O. Bezvikonnyi, D. Volyniuk and J. V. Gražulevičius, *J. Org. Chem.*, 2018, **83**, 1095–1105; (*b*) M. A. Potopnyk, D. Volyniuk, M. Ceborska, P. Cmoch, I. Hladka, Y. Danyliv and J. V. Gražulevičius, *J. Org. Chem.*, 2018, **83**, 12129–12142; (*c*) M. A. Potopnyk, D. Volyniuk, R. Luboradzki, M. Ceborska, I. Hladka, Y. Danyliv and J. V. Gražulevičius, *J. Org. Chem.*, 2019, **84**, 5614–5626; (*d*) M. A. Potopnyk, D. Volyniuk, R. Luboradzki, M. Ceborska, I. Hladka, Y. Danyliv and J. V. Grazulevicius, *J. Org. Chem.*, 2020, **85**, 6060–6072.

15 P. Moonsin, N. Prachumrak, R. Rattanawan, T. Keawin, S. Jungsuttiwong, T. Sudyoadsuk and V. Promarak, *Chem. Commun.*, 2012, **48**, 3382–3384.

16 G. M. Sheldrick, *Acta Crystallogr., Sect. A: Found. Crystallogr.*, 2008, **64**, 112–122.

17 M. J. Frisch, G. W. Trucks, H. B. Schlegel, G. E. Scuseria, M. A. Robb, J. R. Cheeseman, G. Scalmani, V. Barone, B. Mennucci, G. A. Petersson, H. Nakatsuji, M. Caricato, X. Li, H. P. Hratchian, A. F. Izmaylov, J. Bloino, G. Zheng, J. L. Sonnenberg, M. Hada, M. Ehara, K. Toyota, R. Fukuda, J. Hasegawa, M. Ishida, T. Nakajima, Y. Honda, O. Kitao, H. Nakai, T. Vreven, J. A. Montgomery Jr., J. E. Peralta, F. Ogliaro, M. Bearpark, J. J. Heyd, E. Brothers, K. N. Kudin, V. N. Staroverov, T. Keith, R. Kobayashi, J. Normand, K. Raghavachari, A. Rendell, J. C. Burant, S. S. Iyengar, J. Tomasi, M. Cossi, N. Rega, J. M. Millam, M. Klene, J. E. Knox, J. B. Cross, V. Bakken, C. Adamo, J. Jaramillo, R. Gomperts, R. E. Stratmann, O. Yazyev, A. J. Austin, R. Cammi, C. Pomelli, J. W. Ochterski, R. L. Martin, K. Morokuma, V. G. Zakrzewski, G. A. Voth, P. Salvador, J. J. Dannenberg, S. Dapprich, A. D. Daniels, O. Farkas, J. B. Foresman, J. V. Ortiz, J. Cioslowski and D. J. Fox, *Gaussian 09, Revision D.01*, Gaussian, Inc., Wallingford, CT, USA, 2013.

18 L. M. Lifshits, D. S. Budkina, V. Singh, S. M. Matveev, A. N. Tarnovsky and J. K. Klosterman, *Phys. Chem. Chem. Phys.*, 2016, **18**, 27671–27683.

19 X. Yang, R. Lu, F. Gai, P. Xue and Y. Zhan, *Chem. Commun.*, 2010, **46**, 1088–1090.